Earthquake Engineering, Tenth World Conference © 1992 Balkema, Rotterdam. ISBN 90 5410 060 5

Lateral pile response in liquefying sand

Takaaki Kagawa
Department of Civil Engineering, Wayne State University, Detroit, Mich., USA

ABSTRACT: The potential significance of the impact of liquefaction on the dynamic responses of pile foundation has been demonstrated through a numerical study. Due to liquefaction the pile-head acceleration will be amplified or attenuated and the pile-head displacement and the pile moment will be greatly amplified in most cases. These tendencies are expected to be more pronounced when liquefied soils induce flow movements.

1 INTRODUCTION

Liquefaction has been the key cause of damage and failures of foundations for civil engineering structures in major historical earthquakes. Liquefaction may result in loss of bearing capacity, excessive settlement and tilting, and lateral spread and flow of liquefied soils.

Extensive studies have been made since the Niigata and Alaska earthquakes of 1964 to establish reliable procedures for predicting liquefaction potential. Therefore, liquefaction susceptibility of a site can be predicted with reasonable confidence at present. However, rational prediction of the impact of liquefaction on the performance of structural foundations is not possible at present. This is especially true for pile foundations that are installed in loose saturated sand layers.

The major objectives of this paper were to demonstrate the potential significance of the impact of liquefaction on the performance of pile foundation and to improve our understanding of the phenomenon. For this purpose numerical tools were developed and an extensive parametric study was conducted.

This paper presents first the key features of the numerical methods used in this study. This is followed by presentations of major findings from the parametric study.

2 NUMERICAL MODEL

Dynamic response computations of a soil-pile-structure system involved two major steps; free-field response analysis and soil-pile-structure interaction analysis. The free-field response analysis was made with a one-dimensional, nonlinear site-response method SRANG2 and the soil-pile-structure interaction analysis was performed with NONSPS2. The original versions of these programs, SRANG and NONSPS, were developed by Kagawa and Kraft (1981b). These programs have been rewritten and upgraded for this study to incorporate various new features and to increase their computational efficiency. The major features of these numerical methods are highlighted below.

2.1 Free-field response model

Responses of free-field soils against seismic waves were obtained by using the one-dimensional wave propagation theory, which has been used in most site-response analyses. Computed soil responses were used in separate and subsequent soil-pile-structure interaction analyses. The stress-strain relation of soil for the free-field analyses was represented by a one-dimensional simplification of the multi-surface model (Mroz 1967). The backbone curve of the stress-strain relation was determined from a hyperbolic model fit of experimentally determined stress-strain relations of soil.

Excess pore pressures develop in sands during earthquake loading. The pore pressure model developed by Kagawa and Kraft (1981a) was used in the program SRANG2 to evaluate such pore pressures. One-dimensional consolidation model was used to compute redistribution and dissipation of excess pore pressures.

The program SRANG2 included a viscous transmitting boundary at the base of the layered system to model a visco-elastic half space.

2.2 Soil-pile-structure interaction model

The soil-pile-structure interaction model used in this study was based on a beam-on-Winkler foundation model. A pile-supported structural system was represented by a single-pile system. The superstructure was represented by a series of lumped masses, connected by beams, that possess lateral degrees-of-freedom only. The pile was discretized into segments, and each pile segment was connected to free-field soil through discrete soil-pile elements. These discrete soil-pile elements represented: 1) variations of near-field soil properties with depth, 2) nonlinear stress-strain behavior of soils around a pile, 3) three-dimensional soil-pile interaction effects, 4) excess pore pressure build-up in the free field and around a pile and 5) pore pressure dissipation and redistribution into the radial direction away from the pile and into the vertical direction. The key features are summarized below.

2.2.1 Soil reaction to pile

For a pile in linearly elastic soil layers, the lateral soil reaction, p, at some depth on a unit pile length can be approximated by (Kagawa and Kraft 1980, Kagawa 1992):

$$p = E_s\bar{\delta}y + 2\rho_s B(V_s + V_p)\frac{dy}{dt} \qquad .....(1)$$

in which E_s = the representative Young's modulus of soil, $\bar{\delta}$ = the average soil-reaction coefficient that is constant with depth, y = the pile deflection relative to the free-field soil, ρ_s = the mass density of the free-field soil, B = the equivalent width of the pile, and V_s and V_p = the shear and constrained wave velocities of the free-field soil.

The average soil-reaction coefficient, $\bar{\delta}$, can be related to the local soil-pile flexibility factor $\bar{K}_r = EI/(E_s r_o^4)$, as shown in Fig. 1. EI is the flexural rigidity of the pile and r_o is the equivalent pile radius. The velocity-dependent term in Eq. 1 represents the three-dimensional wave energy dissipation away from the pile, using the dashpots that absorb plane shear and constrained waves.

The linear p-y relation in Eq. 1 may be extended to include nonlinear stress-strain behavior of soils. High shear-strain concentration occurs in the vicinity of a pile due to soil-pile interaction, and the nonlinear stress-strain behavior of the soils can have a large impact on pile response.

To represent this effect, this study considered representative behavior of soils around a pile. The pile displacement, y, was related to the representative shear strain of soils, γ, as:

$$\gamma = (1+\nu)y/(fB) \qquad .....(2)$$

in which ν = the Poisson's ratio of soil, and f = the influence factor that depends, for example, on the shape of loaded area, the distribution of soil modulus with depth, and the relative stiffness of the pile to soils. The influence factor, f, of course, varies with depth. A typical value of f is three to five. The shear strain in Eq. 2 may then be used to obtain a representative shear stress in the soil around the pile τ as:

$$\tau = G_s\gamma = G_{max}F(\gamma/\gamma_r)\gamma \qquad .....(3)$$

in which G_s = the representative shear modulus of soil, G_{max} = the shear modulus at very small shear strain, and γ_r = the reference shear strain (= τ_{ult}/G_{max}). τ_{ult} is the apparent shear resistance of the representative soil element around the pile and $F(\gamma/\gamma_r)$ is a strain-dependent function that represents the stiffness degradation with strain amplitude. With Eqs. 2 and 3, the lateral soil reaction in Eq. 1 for linearly elastic soil layers may be rewritten for nonlinear stress-strain conditions as:

$$p = 2f\bar{\delta}B\tau_{ult}F(y^*)y^* + 2\rho_s B(V_s + V_p)\frac{dy}{dt} \quad .....(4)$$

in which the normalized pile deflection y^* is defined as $(1+\nu)y/(fB\gamma_r)$. The apparent shear resistance of soil around the pile, τ_{ult}, may be determined by considering the passive failure of the soil element adjacent to a pile as:

$$\tau_{ult} = A(\bar{\sigma}_v \sin\bar{\phi} + \bar{c}\cos\bar{\phi})/(1-\sin\bar{\phi}) \quad .....(5)$$

in which A = an empirical adjustment factor, which was assumed to be unity in this study, $\bar{\sigma}_v$ = the effective overburden stress, and $\bar{\phi}$ and $\bar{c}$ = the static strength parameters of soil.

2.2.2 Excess pore pressure generation

Excess pore pressures develop in the soils around a pile due to pile displacements relative to those of free-field soils. The effects of these excess pore pressures and associated degradation of soil stiffnesses were accounted for by successively modifying the stiffnesses and strengths of near-field and free-field soils. This was accomplished by applying a factor $(1-r)^{\alpha}$ on the stiffnesses and strengths of the soil-pile elements. r is the pore pressure ratio given as the ratio between excess pore pressure and the initial effective overburden stress. α is a coefficient that depends on soil type; a typical value for sands is 0.5.

After complete liquefaction soil was assumed to provide viscous resistance to pile movements.

2.2.3 Excess pore pressure redistribution

Excess pore-water pressures develop in soils around a pile due both to free-field ground movements and to the relative movements between the soils and the pile. The former type of pore pressures redistribute in the vertical direction, while the latter type of pore pressures redistribute in both the vertical and radial directions. Therfore, the soil-pile-structure interaction model included an axisymmetric, finite-element consolidation model that handles coupled flow of these two types of pore pressure redistribution.

3 PARAMETER STUDY

A parametric study was conducted to evaluate and demonstrate the impact of liquefaction on the earthquake responses of a single-pile system. The soil-pile-structure systems studied are shown in Fig. 2. The radius of the pile is 0.5 ft; its length is 100 ft; the pile carries a concentrated structural weight of ; and the bottom 60 ft of the pile is embedded into clay. In CASE I the top 40 ft of the pile is supported by loose saturated sands, while CASE II and III have fill layers with thicknesses of 10 ft and 30 ft, respectively. The ground water table was assumed at the top of the loose saturated sand layers.

In addition to the soil-pile-structure conditions presented in Fig. 2, the following conditions were also analyzed; 1) no liquefaction in sand layers and 2) no soil in the top 40 ft of the pile. These cases provided measures of the significance of the impact of liquefaction on pile responses.

Responses of the soil-pile-structure systems were computed for sinusoidal shear-wave excitations and for selected earthquake motions. Twenty historically recorded earthquake records were used in this study. These records included four motions from the Loma Prieta earthquake, seven Japanese motions, and western U.S.A. motions. The acceleration amplitudes of these records were scaled to four levels, ranging from 0.05 g to 0.40 g.

4 RESULTS

4.1 Steady-state responses

Figure 3 shows the frequency responses of pile-head accelerations and of the maximum moments in pile for CASE I with 0.05 g excitations. As indicated in Fig. 3, the soil-pile-structure system has a resonant frequency at about 0.6 Hz when the top 40 ft of sand liquefies. Since the excitation level was low, the top

40 ft of sand didn't liquefy completely. Therefore, the pile-head accelerations and the maximum moments in pile were reasonably close to those for no liquefaction cases.

Figure 4 shows similar results for 0.15 g excitations. Complete liquefaction of the top 40 ft of sand took place at all frequencies. The pile-head accelerations and the maximum pile moments are given as envelopes of those for the no liquefaction and no sand layer cases.

4.2 Earthquake responses

Typical results obtained from this analysis are shown in Fig. 5.

Figures 6 through 8 summarize results for maximum pile-head accelerations, maximum pile-head displacements, and maximum pile moments for all the conditions of CASE I. Figure 6 shows that the pile-head accelerations for the no liquefaction cases are nearly uniquely related to corresponding free-field surface accelerations. The pile-head accelrations for the liquefaction cases, however, may be amplified or attenuated from those of the no liquefaction cases. The degree of amplification or attenuation is shown to be larger at higher free-field acceleration levels. Figures 7 and 8 demonstrate the significance of liquefaction on pile foundation design. Figure 7 shows the peak pile-head displacement for the liquefaction case normalized by that for the no liquefaction case. Figure 8 shows similar ratios for the maximum pile moments. Liquefaction is shown to result in significant increase in pile movement and moment due to loss of lateral soil support.

The results presented above are for CASE I. The impact of liquefaction on pile responses in this case was larger than that of the other cases.

5 CONCLUSIONS

The potential significance of the impact of liquefaction on the performance of pile foundation has been demonstrated. Due to liquefaction the pile-head acceleration will be amplified or attenuated and the pile-head displacement and the pile moment will be greatly amplified in most cases. These tendencies are expected to be more pronounced when liquefied soils induce flow movements.

REFERENCES

Kagawa, T. 1992. Modeling the soil reaction to laterally loaded piles. *71st Transportation Research Board Annual Meeting, Transportation Research Board*, Washington, D.C.

Kagawa, T. and Kraft, L.M., Jr. 1980. Lateral load-deflection relationships of piles subjected to dynamic loadings. *Soils and Foundations, Japanese Society of Soil Mechanics and Foundation Engineering*, Vol.20, No.4, 19-36.

Kagawa, T. and Kraft, L.M., Jr. 1981a. Modeling the liquefaction process. *Journal, Geotechnical Engineering Division, ASCE*, Vol.107, No.GT12, 1593-1607.

Kagawa, T. and Kraft, L.M., Jr. 1981b. Lateral pile response during earthquakes. *Journal, Geotechnical Engineering Division, ASCE*, Vol.107, No.GT12, 1713-1731.

Mroz, Z. 1967. On the description of anisotropic work hardening. *Journal, Mechanics and Physics of Solids*, Vol. 15, 163-175.

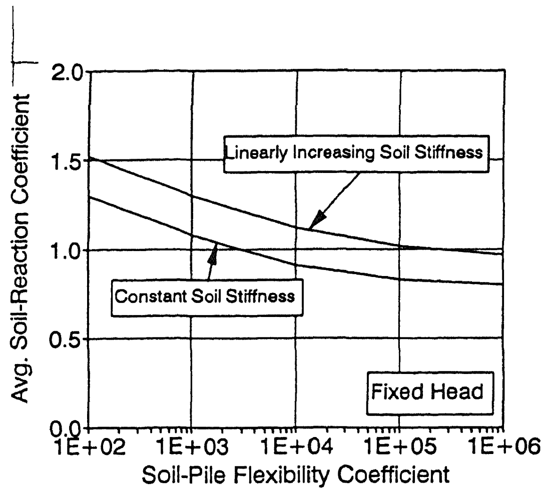

Fig. 1 Soil-Reaction Coefficient

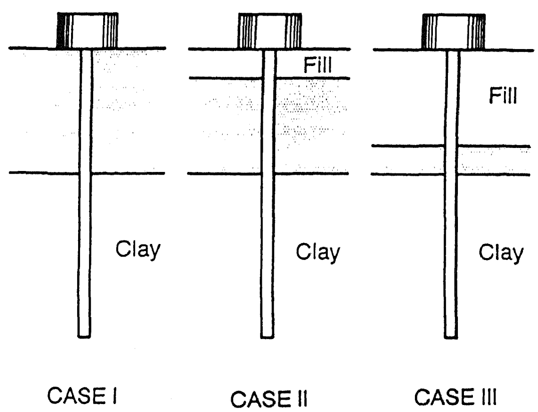

Fig. 2 Soil-Pile Conditions for Study

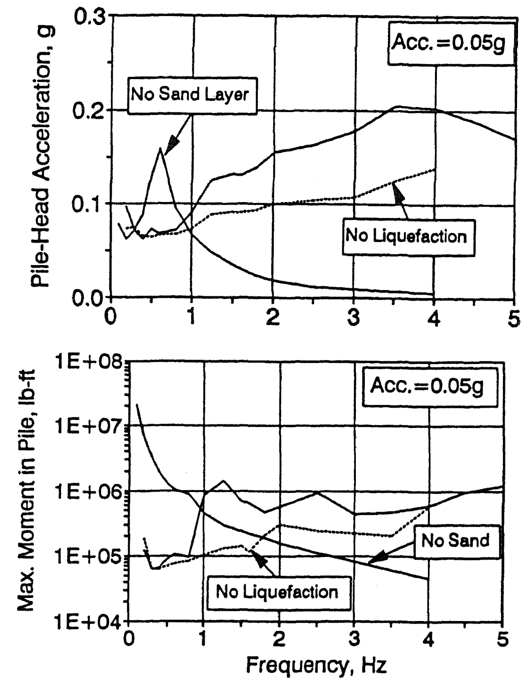

Fig. 3 Steady-State Responses
(CASE I, 0.05 g Excitation)

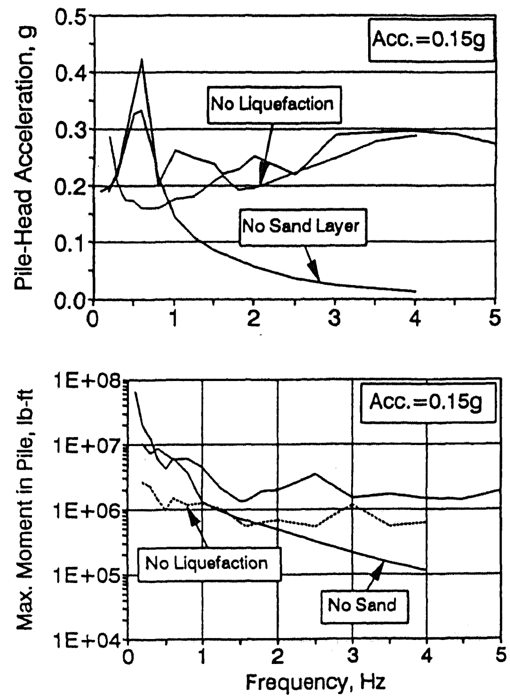

Fig. 4 Steady-State Responses
(CASE I, 0.15 g Excitation)

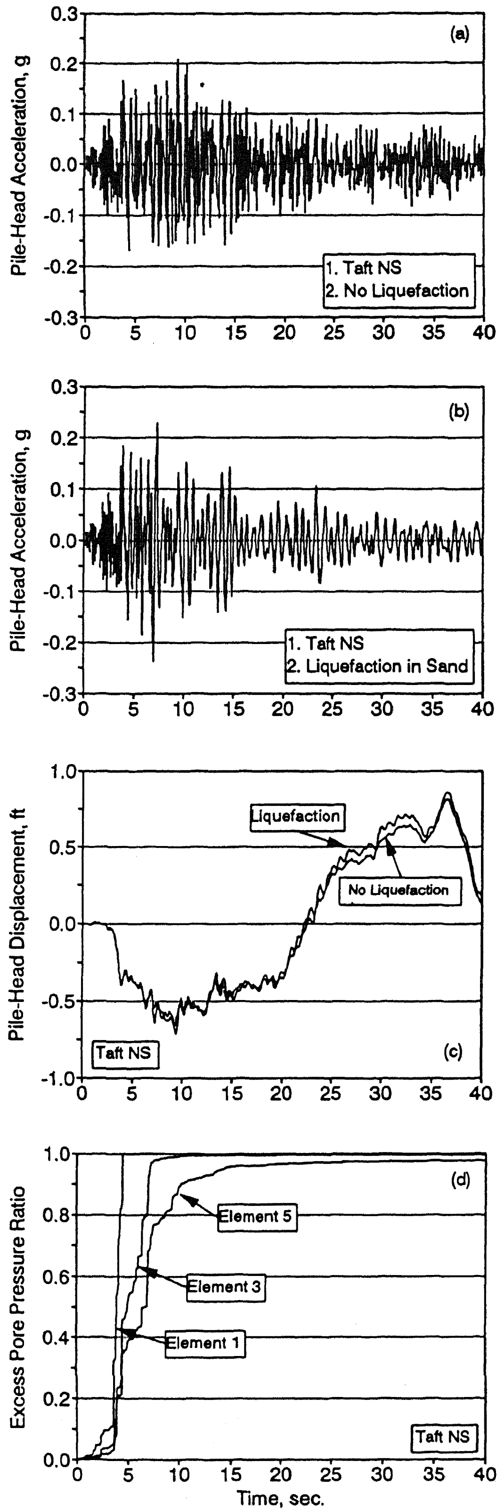

Fig. 5 Typical Earthquake Responses

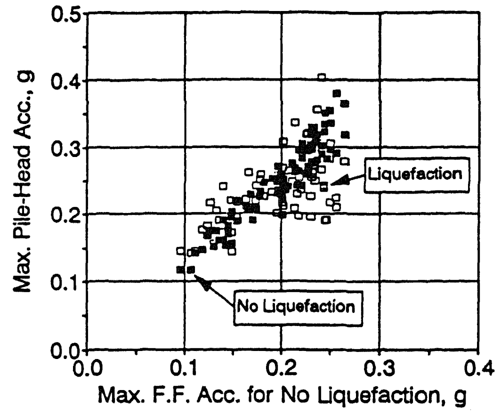

Fig. 6 Pile-Head Accelerations for Earthquake Loading

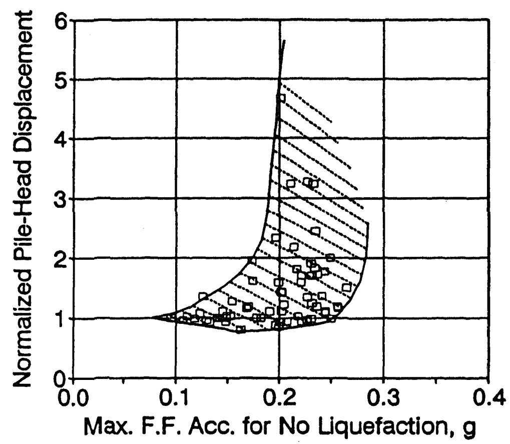

Fig. 7 Pile-Head Displacements for Earthquake Loading

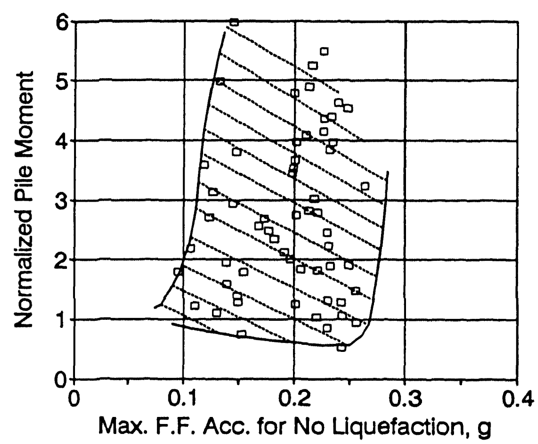

Fig. 8 Pile Moments for Earthquake Loading